A Multiphase Fluid Mechanics Approach to Gas Holdup in Bath Smelting Processes

H. GOU, G.A. IRONS, and W.-K. LU

In slag-based, smelting-reduction processes, the overflow of slag from the vessel is considered a major limitation to productivity; this phenomenon is commonly called slag foaming. While much has been learned from laboratory-scale studies of foaming, the superficial gas velocities are well below those encountered in production (centimeters per second compared to meters per second). A multiphase fluid dynamic model was developed to determine the relationship between gas velocity and void fraction (holdup) at industrial production rates. In the model, the drag between the gas and slag is balanced against the weight of the slag. Within the framework of the model, the only unknown quantity is a drag factor which can be extracted from experimental data. Values of this factor from water models, smelting-reduction converters, and other slag systems fall in a narrow range. The model can be used to estimate slag height in smelting-reduction vessels. The behavior of slags at high rates of gas injection is markedly different from foaming observed at low flow rates.

I. INTRODUCTION

In several new smelting-reduction processes for ironmaking, coal and partially prereduced iron ore are added to a slag phase.[1,2,3] The iron oxide quickly dissolves in the slag to be reduced by the coal,

$$(FeO) + C_{(s)} \Rightarrow Fe + CO \qquad [1]$$

to produce iron that collects at the bottom of the vessel. Reduction can also be accomplished by carbon dissolved in iron by a similar reaction:

$$(FeO) + \underline{C} \Rightarrow Fe + CO \qquad [2]$$

Oxygen is delivered by a top oxygen lance which combusts the carbon (and other volatile hydrocarbons) in the coal:

$$2C_{(s)} + O_2 \Rightarrow 2CO \qquad [3]$$

In a similar manner to oxygen steelmaking, oxygen will also be absorbed into the slag where it will react by equations similar to Eqs. [1] and [2] to form carbon monoxide. Unreacted oxygen, or oxygen introduced later, reacts with the evolved carbon monoxide to produce carbon dioxide (postcombustion),

$$2CO + O_2 \Rightarrow 2CO_2 \qquad [4]$$

that generates additional heat for the process.

The objective of these new ironmaking processes is to supplant conventional blast furnaces by much smaller, more intensive reactors. Consequently, the intensity of gas evolution in the slag is unprecedented in a metallurgical reactor. The slag layer is lifted due to this extremely high gas evolution rate and may even flow over the top of the vessel; this phenomenon is commonly called slag foaming. It is generally accepted that slag foaming is one of the key limiting factors in the development of these new processes.[4-7] Recently, there have been several studies on the slag foaming phenomenon related to the smelting-reduction processes, both in laboratory-scale furnaces[8-14] and in operational smelters.[15,16] In some laboratory-scale studies, the foaming was generated by passing an inert gas through a molten slag layer at low flow rate.[8-11] In others, the gas was generated from reduction reactions taking place between iron oxide-containing slag and carbonaceous materials.[12,13,14] In these studies, the superficial gas velocities (volumetric flow rate per unit cross-sectional area of the vessel) were of the order of a few centimeters per second. X-ray photographs clearly show that the foams resemble soap or beer bubble foams.[13] It was found that the extent of foaming depended on the superficial gas flow rate and slag properties, particularly slag viscosity and surface tension.[8,9,10,13,14]

Ogawa *et al.*[14] investigated gas bubble formation and size in a foaming slag to understand foaming phenomena and control. Based on experimental evidence and a static force balance between buoyancy and surface tension forces, they developed models to calculate the gas bubble size and the void fraction in the foam layer. The conclusion of these studies was that the foaming behavior was only related to slag chemistry, viscosity, and surface tension. It is difficult to directly relate these static force balances to foaming in very intense smelting-reduction processes. In an attempt to develop the fluid dynamic aspects of slag foaming, they used the Wallis[17] approach to analyze their experimental results. Wallis' approach is simply a one-dimensional mass balance for the two phases in the system which requires experimental knowledge of the fluxes of both phases. Ogawa's work was conducted in the laboratory, so it is unclear how to extrapolate the analysis to industrial-scale vessels.

Most recently, Lin and Guthrie investigated foaming with low-temperature models in which the superficial velocity of the gas was less than 0.15 m/s.[18] They concluded that the behavior of the bubbles was quite different at low flow rates from that in the churn-turbulent regime.

In industrial smelting-reduction furnaces, large quantities of gas are introduced into and generated within the slag

H. GOU, formerly Research Associate with the Department of Materials Science and Engineering, McMaster University, is Process Engineer with Hatch Associates Ltd., Mississauga, ON, Canada L5K 2R7. G.A. IRONS, Dofasco/NSERC Professor of Process Metallurgy, and W.-K. LU, Professor, are with the Department of Materials Science and Engineering, McMaster University, Hamilton, ON, Canada L8S 4L7.

Manuscript submitted July 20, 1993.

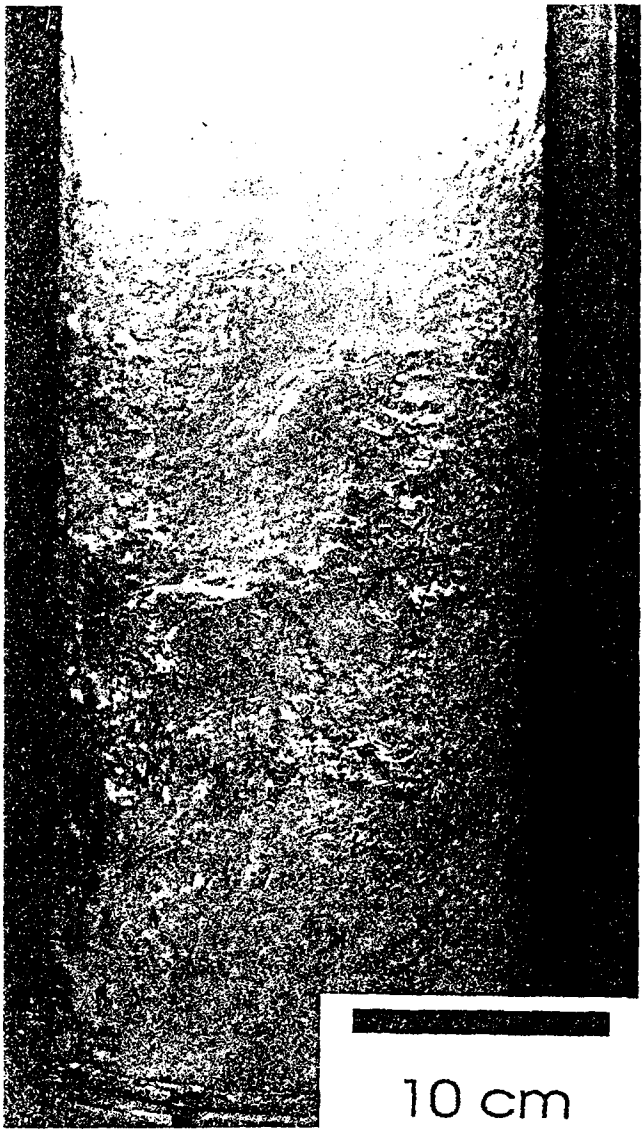

Fig. 1—Photograph of column containing water with air injected at a superficial gas velocity of 3.05 m s^{-1} and void fraction of 0.78, courtesy of E. Aida and A. Kapoor, McMaster University.

layer, as described previously. Depending on the operating conditions and raw materials used, gas generation rates are in the range of 1200 to 2000 Nm^3/tonne of hot metal, resulting in superficial velocities of several meters per second which are two orders of magnitude greater than in the laboratory studies. The slag height has been reported as a function of smelting rate and the coke/slag ratio. Generally, it has been found that the slag height increases with production rate, and that coke or char significantly reduces slag height, and is thus an important means to control slag height. No models have been proposed for calculating slag height at such high rates of gas evolution nor is it clear how the models validated at low flow rate may be extrapolated to industrial conditions.

In the present work, a fluid dynamics approach is applied to multiphase systems operating at much higher flow rates than that normally considered slag foaming. The model provides a framework for analyzing data from experiments. A reasonably consistent picture emerges after examination of data from pilot-scale smelting-reduction vessels, water models, and experiments in other molten oxide systems.

II. MATHEMATICAL MODEL

The objective of the present work is to develop a model of the slag layer in smelting-reduction furnaces where the superficial gas velocities are of the order of meters per second; the model can calculate the void fraction (or holdup). Frank *et al.*[19] constructed a simple water column with a sieve plate at the bottom to distribute injected gas uniformly at superficial gas velocities up to 3 m/s. The water was agitated in a very turbulent manner with irregularly shaped bubbles, roughly 100 mm, rising in the vessel. A similar column was constructed in the authors' laboratory, Figure 1 is a photograph taken of high-velocity injection. There was no noticeable gradient in void fraction from the top to the bottom nor was there a significant amount of beer bubblelike foam. In multiphase flow literature, this regime is called the churn-turbulent regime.[20]

It is instructive to examine the chemical and mechanical engineering literature related to multiphase flow. Shah *et al.*[21] prepared a comprehensive review of flow in bubble columns. However, the results are not directly applicable because the superficial velocities were less than 1 m/s. They considered that the empirical correlations of Akida and Yoshida[22] and Hikita *et al.*[23] were the most reliable. Both these correlations are restricted to velocities less than 0.4 m/s:

$$\theta = 0.672\ u_s^{0.578}\ \rho_l^{0.069}\ \mu_l^{-0.053}\ \rho_g^{0.062}\ \mu_g^{0.107}\ \sigma^{-0.185}\ g^{-0.131} \quad [5]$$

and

$$\frac{\theta}{(1-\theta)^4} = 0.2\ u_s^{1.0}\ \rho_l^{0.292}\ \mu_l^{-0.167}\ \sigma^{-0.125}\ g^{-0.292} \quad [6]$$

From examination of the coefficients in both of these equations, it is clear that void fraction depends primarily on the superficial gas velocity and is only weakly dependent on the physical properties of the gas and liquid. These correlations apply in the churn-turbulent regime, where large irregularly shaped bubbles rise in a very agitated vessel, such as in Figure 1. Clearly, these are not the classical foams, like beer or soap bubbles. In fact, most of the liquids were pure which means they cannot foam in the classical manner. It was also found that when small solid particles were present in the column, these correlations were also applicable, if the solid densities were close to water.

Kozakevitch[24] pointed out in his authoritative review of foams and emulsions in steelmaking processes that as the gas supply to the slag layer becomes very large, even nonfoaming slags will foam. In other words, the slag cannot create a stable, classical foam but can be expanded by very high gas flow rates.

It is our contention that when the superficial velocity is greater than approximately 1 m/s, the holdup of gas is primarily governed by gravity and the drag forces that the gas exerts on the liquid. Thus, the system will appear as shown in Figure 1. It will be shown that a wide variety of physical systems operate in this manner. Further work will be required to clarify the dependence on the physical properties, but it is expected to be even weaker than Eqs. [5] and [6] as the gas flow rate increases.

A. *Assumptions*

The mathematical model developed here to calculate the liquid height and void fraction is a one-dimensional, fluid mechanical model for gas and liquid two-phase flow. It is assumed that the cross-sectional area of the vessel is much larger than the bubble size, so that the gas and liquid fractions can be averaged across the vessel. On the other hand, the bubbles are at least several centimeters in diameter, so that surface tension forces can be ignored in the momentum balance.

It is also assumed that in the cases where there is a top jet present, it has little effect on the liquid height. It has been shown previously that top jets may penetrate locally into a liquid, but that the kinetic energy of the jet is poorly coupled to the liquid. Conversely, the potential energy of submerged gas or gas generated under the liquid surface is much larger and well coupled to the liquid.[25] Therefore, the submerged gas will dominate the flow in the liquid.

The other assumptions used in the modeling are as follows:

(1) the gas is ideal;
(2) the liquid is incompressible;
(3) there is no liquid flow from the system, so the total liquid mass is conserved;
(4) once the gas is generated, there are no further chemical reactions involved in the system;
(5) the gas and liquid are in thermal equilibrium;
(6) viscous dissipation is ignored; and
(7) the system is at steady state.

B. *Mathematical Formulation*

The model is similar to other one-dimensional models developed by Farias and Irons[26] for gas injection into ladles and more recently by Hanumanth *et al.*[27] for sedimentation of particles in metal-matrix composites. Since there is no liquid flowing from the system, the net liquid velocity is zero. In this model, equations are written for mass and momentum conservation in the vertical direction for gas phase only. The equations are averaged over the cross section of the vessel.

The gas continuity equation,

$$\frac{d}{dz}(\rho\theta u) = 0 \qquad [7]$$

simply states that the mass flux is unchanged in the vertical direction. The momentum equation for the gas phase shows that the acceleration of the gas is due to the balance of the buoyancy and drag forces:

$$\frac{d}{dz}(\rho\theta u^2) = F_B - F_D \qquad [8]$$

The buoyancy force is

$$F_B = (\rho_l - \rho)g\theta \qquad [9]$$

The form of the interphase drag force between gas and liquid,

$$F_D = \frac{3}{4}\frac{C_D}{d_B}u^2\,\rho_m\theta = f_D u^2\,\rho_m\theta \qquad [10]$$

is based on the force on a single bubble multiplied by the number of bubbles in the cross-sectional area. Since neither the bubble diameter nor the drag coefficient is known *a priori*, it is convenient that they appear together in f_D, which will be called the drag factor in the following discussion.

The mixture density is defined as

$$\rho_m = \rho\theta + \rho_l(1-\theta) \qquad [11]$$

in which the local gas density is calculated from

$$\rho = \frac{PM}{RT} \qquad [12]$$

The total pressure, P, is the hydrostatic pressure due to the mixture

$$P = P_{atm} + g\rho_m(h_f - z) \qquad [13]$$

where h_f is the total mixture height.

It is assumed that the vessel is tall enough that no liquid is lost from the system. Consequently, the weight of the liquid is conserved before and during gas injection which is expressed mathematically as

$$W_l = A\int_0^{h_f}\rho_l(1-\theta)\,dz = Ah_0\rho_l \qquad [14]$$

Equations [7] through [10] can be manipulated to obtain the differential equation for the gas velocity over the vessel height:

$$\frac{du}{dz} = \frac{g(\rho_l-\rho)}{u\rho} - \frac{f_D u\rho_m}{\rho} \qquad [15]$$

The gas void fraction is determined from the relation

$$\theta = u_s/u \qquad [16]$$

where u_s is the superficial gas velocity.

C. *Solution of Equations*

Solution of the problem requires that Eqs. [14] through [16] be solved simultaneously. To do so requires knowledge of the drag factor, f_D, which contains the drag coefficient, C_D, and the effective bubble diameter, d_B (Eq. [10]). Values of f_D will be extracted from experimental data in Section D. In this section, some of the basic features of the solutions are examined.

The gas velocity, u, is obtained by solving Eq. [15] by the Runge–Kutta method. The void fraction is then calculated with Eq. [16]. Figure 2 shows example calculations for typical smelter conditions; the superficial gas velocity was calculated from the gas evolution rate due to smelting. The gas is introduced at $z = 0$; it is apparent that the gas velocity and void fraction quickly adjust themselves so that the velocity and void fraction curves are virtually straight lines through the remaining rise. This finding indicates that the flow is dominated by the balance between the interphase drag force and the buoyancy force; the initial momentum is quickly dissipated. The sensitivity of the solutions to the initial conditions for void fraction and velocity was examined; again, it was found that these quantities quickly rearranged themselves to the same solution regardless of the initial conditions. (Of course, Eq. [16] shows that the product of the void fraction and gas velocity must be the superficial velocity.) Because the initial conditions have such

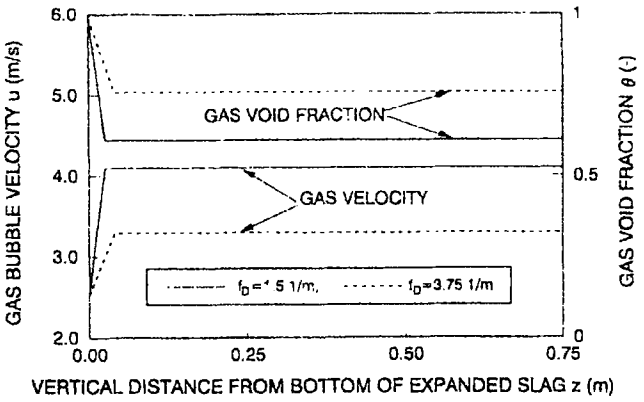

Fig. 2—Calculated gas velocity and void fraction along the expanded slag layer height for the following conditions: h_0 = 0.5 m, u_g = 2.5 m s^{-1}, ρ_l = 3000 kg m^{-3}, and T_g = 1500 °C.

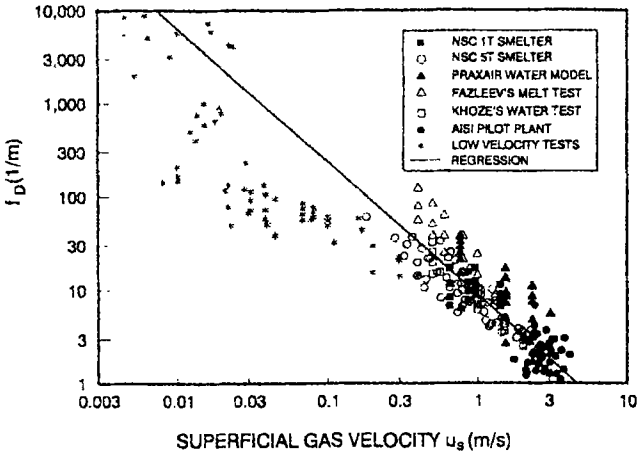

Fig. 3— Calculated drag factors based on the experimental measurements of liquid/gas mixture height against superficial gas velocity.

a small effect on the solutions, this model may be applied to different systems where the gas is generated inside the system, such as in a smelter, or introduced into the system by injection.

D. *Estimation of the Drag Factor*

The values of the drag factor, f_D, were extracted from measured liquid expansion heights or gas void fraction values by solving Eq. [15] and adjusting f_D to satisfy Eq. [14], the conservation equation for liquid mass. As noted in Section C, the void fractions were virtually constant after a short initial adjustment distance. Several liquid expansion height measurements are available in the literature where the superficial gas velocities are close to those in bath smelters. A good systematic study of slag expansion height under different smelting rates was reported by Hirata *et al.* of Nippon Steel Corporation (NSC).[15] The experiments were carried out in a 1 tonne smelter with continuous ore/coke feeding and oxygen blowing. The smelting rates were converted to equivalent superficial gas velocities, assuming all the reduced iron oxide resulted in carbon monoxide formation in the slag.

Tokumitsu and colleagues, also from NSC, reported the measured slag height against the total iron content in the slag in both 1 and 5 tonne smelters.[16] From the relationship between the iron content in the slag and the rate of oxygen supply from the iron ore, the relationship between the slag height and the superficial gas velocity was obtained.

In the American Iron and Steel Institute (AISI) Direct Steelmaking program, slag heights were measured in the pilot plant smelters.[28] Some of the data taken from a 5 tonne converter-type smelter are used in this study. The gas evolution rate in the slag was calculated based on the iron ore and coal charging rates, the oxygen blowing rate, and the off-gas composition. Also, under the AISI program, Frank *et al.* of Praxair Inc. conducted a series of experiments in a water tank where nitrogen or helium was injected from the bottom at high gas flow rate.[19] The corresponding mixture heights were recorded.

There are two other studies at high gas flow rate by investigators in the former Soviet Union. Fazleev *et al.*[29] measured the average gas void fraction in a K_2O-V_2O_5 melt with superficial gas velocities up to 1 m/s. Khoze *et al.*[30] measured average void fractions with superficial gas velocities from 0.5 to 2.5 m/s in a water model.

For comparison, three experiments at low gas velocities are also included. Ito and Fruehan[8] studied foams of CaO-SiO_2-FeO slags generated by introducing argon into the molten slag in an alumina crucible. The foam heights were measured by an electric probe. In a small graphite crucible, Kitamura and Okohira[12] observed slag foaming caused by reactions between iron oxide-containing slag and hot metal for various temperatures and slag compositions; the measured foaming slag height against CO gas generation rate was reported. Yoshita and Akita[31] conducted experiments by injecting gas, air, or oxygen into a liquid column containing sodium sulfite solution, at a superficial gas velocity ranging from 0.001 to 0.25 m/s. The measured void fraction against superficial gas velocity was also reported.

All the data treated by the model are plotted in Figure 3; note that it spans three orders of magnitude of superficial gas flow rate. At low flow rates, there is considerable difference from system to system; however, at high flow rates, all the data converge to one line. This is indicative of the fact that at low velocity, the foam and foam height depend on the physicochemical properties of the liquid, but much less so for the expanded liquid at higher gas velocity. Thus, a logarithmic regression between the drag factor and the superficial velocity be extracted from these high gas velocity experiments:

$$\log f_D = 0.95 \pm 0.23 - (1.43 \pm 0.06) \log u_s \quad [17]$$

with $r^2 = 0.74$.

The utility of the model is demonstrated in Figure 4 in which the measured and calculated heights of slag layer are shown for the AISI Direct Steelmaking reactor over a period of time. The superficial velocity was calculated from the mass balance for the vessel which changed over time. Reasonable agreement is achieved, this is to be expected because the AISI data in Figure 3 fall close to the regression line.

III. DISCUSSION

The experimental systems and conditions investigated were quite diverse; they included industrial-scale smelting-reduction processes, gas passing through water tanks, and

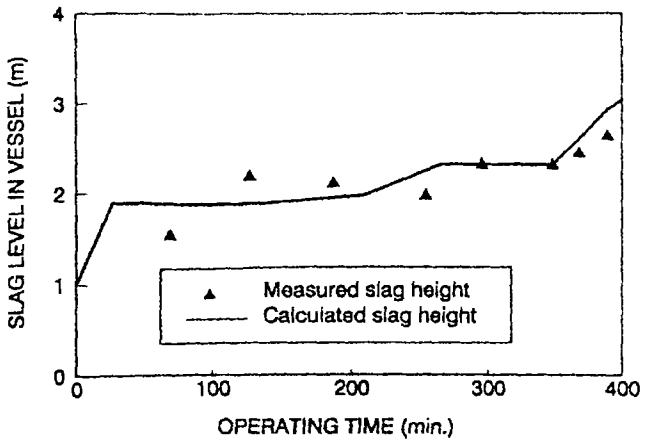

Fig. 4—Comparison of the slag height from measurements in the AISI pilot plant smelter and the modeling results.

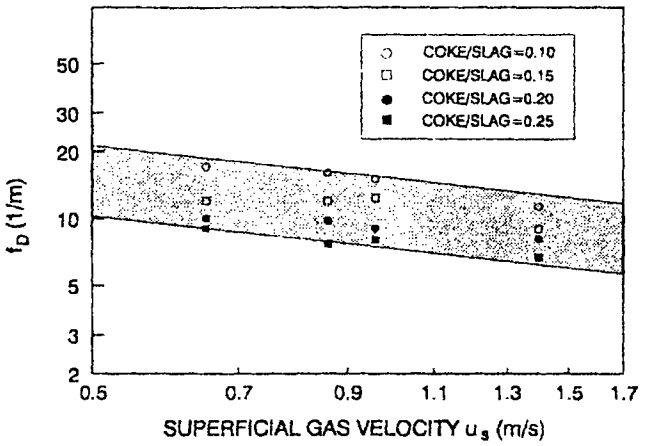

Fig. 5—The influence of the coke/slag ratio on the calculated drag factors from the Nippon Steel Corporation 1 tonne smelter data.

gas introduced into a molten oxide. The gases included CO, O_2, N_2, He, and air, and the temperatures of the systems varied from room temperature up to about 1600 °C. Nevertheless, values of the drag factor, f_D, are all in a narrow band in Figure 3. Closer examination of Figure 3 reveals that there are systematic differences among the various groups of data. It is expected that most of the differences are due to different physical properties of the systems, but this must be confirmed by further work. As mentioned earlier, it is expected that the dependence on physical properties will be small, comparable to those obtained in aqueous systems at lower velocities, such as Eqs. [5] and [6].

One important condition that has been clearly reported is the coke/slag ratio in the slag. Data reported for the NSC 1 tonne smelter are included in Figure 3. That same data are reproduced in Figure 5 where it is seen that the variation is due to different coke/slag ratios. Thus, more precise regressions can be developed, including the coke/slag ratio as a variable. It has been observed by many operators that higher coke/slag ratios depress the slag height; in fact, this is one of the means used to control the process. In terms of the model, the gas finds it way through the slag without lifting the slag as high; *i.e.*, the C_D/d_B or f_D values are lower at higher coke/slag ratios. The present model does not elucidate the mechanisms of this interaction, but it may be hypothesized that the effective bubble diameter increases at higher coke/slag ratios. Ogawa *et al.*[6] showed by X-ray photography that coke serves as a site for coalescence of gas bubbles. For the same gas flow rate, larger bubbles exert less total drag on the slag, and therefore less expansion, which qualitatively supports the hypothesis.

One shortcoming of the present model, and indeed all other models of gas injection into melts, is that the free surface is poorly represented.[32] There is a disengagement region at the free surface which fluctuates considerably, so that the time-average void fraction should increase gradually with height rather than as a step function in the present model.

There are considerable differences between the behavior of the slag observed at low and high superficial gas velocities. For convenience, we call these foaming slags and expanded slags, respectively, as summarized in Table I. From X-ray observations, foaming slags appear like beer or soap foams, having a thin-walled, cellular structure. The foam

Table I. Comparison of Slag Behaviour

Characteristic	Foaming Slag	Expanded Slag
Schematic Drawing	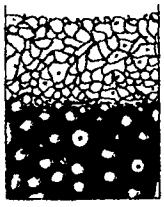	
Appearance	Like beer or soap foam	Turbulent, churning
Uniformity	Two distinguishable layers	One uniformly mixed layer
Gas velocity	0.01 - 0.10 m/s	>1 m/s
Void fraction	0.8 - 0.9	Varies with velocity
Foam height	Independent of total liquid volume	Dependent on the total liquid volume
Stability	Takes time to collapse	Collapses immediately

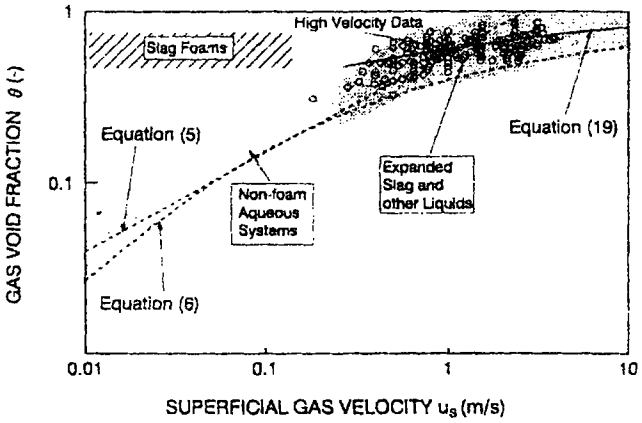

Fig. 6—Relationship between superficial gas velocity and void fraction for three groups of data: slag foams from small-scale experiments, nonfoaming aqueous systems from Shah's review,[21] and the data from the present work, including Eq. [19].

layer forms above a denser layer of slag which has a much lower void fraction. The foam height will not increase even if the depth of the lower layer is increased. If the gas is suddenly turned off, the foam will collapse slowly over a few seconds as the film walls rupture. This regime has been observed at superficial velocities between 0.01 and 0.1 m/s. In contrast, the expanded slags occur at much higher superficial velocities, 1 to 10 m/s, that are characteristic of smelter operations. From water model observations, the entire volume of the liquid is uniformly expanded in a turbulent, churning manner. Katayama *et al.* used an optical fiberscope to look directly inside the slag layer of an operating 100 tonne smelting-reduction vessel.[33] At low rates of gas generation, they found that the slag was composed of two layers, a dense layer under a foamy layer. At higher rates of gas generation, characteristic of practical smelting conditions, there was only one layer.[34] These findings strongly support the present arguments. In the expanded slag regime, increasing the superficial velocity will increase the mixture height and the void fraction. Similarly, increasing the liquid volume will increase the mixture height. If the gas is stopped, the slag will collapse immediately because it does not have the thin-walled, cellular structure of the foam. Expanded slag may be considered more like "fluidized" slags, analogous to fast fluidized beds of solids.

As shown in Figure 2, the gas velocity and void fraction are virtually constant throughout the expanded slag; Eq. [15] may be simplified by setting du/dz to zero. Because the gas density is much less than that of the liquid, $(\rho_l - \rho) \approx \rho_l$ and $\rho_m \approx \rho_l(1 - \theta)$, this permits further simplification of Eq. [15] to

$$f_D = \frac{g\theta^2}{u_s^2\,(1 - \theta)} \qquad [18]$$

$$\frac{\theta^2}{(1 - \theta)} = 0.91\ u_s^{0.57} \qquad [19]$$

Combining Eq. [18] with the regression equation for the data (Eq. [17]) to eliminate f_D, a simple expression between superficial gas velocity, u_s, and gas void fraction, θ, is obtained. One may use this relation as a simple estimate for the holdup in expanded, churned liquids at high gas velocities rather than solve the differential equations.

Equation [19] is plotted in Figure 6, along with the range of the data used to develop it. Equations [5] and [6] are also presented in the hatched region which represents the range of data for nonfoaming aqueous systems.[21] The two sets of data are apparently continuous, but the slope is lower at higher velocities. Foaming slags, observed at low superficial velocities, have void fractions between 0.7 and 0.9;[9] these data appear in the upper left corner of Figure 6. It is clear that the foaming regime is distinctly different from the other two regimes.

IV. CONCLUSIONS

A one-dimensional, multiphase, fluid dynamic model was developed to determine the relationship between superficial gas velocity and void fraction (holdup) in liquids when gases are injected at high rates. The model, based on the balance of drag forces and gravity, requires knowledge of a drag factor that can be extracted from experimental data. Values of this factor for smelting-reduction vessels, water models, and other slag systems fall in a narrow band. This model, using these factors, can be used to calculate slag heights in smelting-reduction vessels. The behavior of the slags subjected to high rates of gas injection, greater than 1.0 m/s, is distinctly different from classical foaming observed at low rates of injection, below 0.1 m/s.

ACKNOWLEDGMENTS

Support of this work was provided by the AISI-DOE Direct Steelmaking Program, 77 pct funded by the United States Department of Energy and the balance by the American Iron and Steel Institute. The authors wish to thank M. Schlichting, K. Downing, and E. Aukrust, AISI Direct Steelmaking, and R. Frank, R. Selines, and Z. Du, Praxair Inc., for allowing us to use their unpublished research data in this work.

NOMENCLATURE

A	area (m^2)
C_D	drag coefficient (−)
d_B	gas bubble diameter (m)
f_D	drag factor, defined in Eq. [10] (m^{-1})
F_B	buoyancy force on the gas bubble (N m^{-3})
F_D	drag force (N m^{-3})
g	gravitational acceleration (m s^{-2})
h_o	liquid height before gas injection (m)
h_f	gas-liquid mixture height (m)
M	gas molecular weight (kg $kmol^{-1}$)
P	pressure (N m^{-2})
R	gas constant (J mol^{-1} K^{-1})
T	temperature (K)
u	gas velocity (m s^{-1})
u_s	superficial gas velocity (m s^{-1})
W	mass (kg)
z	vertical distance from bottom (m)
θ	gas void fraction or holdup (—)
μ	viscosity (kg m^{-1} s^{-1})
ρ	density (kg m^{-3})
σ	surface tension (kg s^{-2})
Subscripts	
atm	atmospheric
B	gas bubble
g	gas
l	liquid
m	mixture

REFERENCES

1. K. Saito: *Proc. Savard/Lee Int. Symp. on Bath Smelting*, TMS, Montreal, 1992, pp. 579-90.
2. E. Aukrust: *Proc. Savard/Lee Int. Symp. on Bath Smelting*, TMS, Montreal, 1992, pp. 591-610.
3. T. Ibaraki, M. Kanemoto, S. Ogawa, H. Katayama, and H. Ishikawa: *I&SM*, 1990, Dec., pp. 30-37.
4. M. Tokuda and S. Kobayashi: *Proc. 7th Process Technology Conf.*, ISS-AIME, Toronto, 1988, pp. 3-11.
5. S. Hara and K. Ogino: *Iron Steel Inst. Jpn. Int.*, 1992, vol. 32, pp. 81-86.
6. Y. Ogawa, H. Katayama, H. Hirata, N. Tokumitsu, and M. Yamauchi: *Iron Steel Inst. Jpn. Int.*, 1992, vol. 32, pp. 87-94.

7. R. Jiang and R.J. Fruehan: *Metall. Trans. B*, 1991, vol. 22B, pp. 481-89.
8. K. Ito and R.J. Fruehan: *Proc. 7th Process Technology Conf.*, ISS-AIME, Toronto, 1988, pp. 13-21.
9. K. Ito and R.J. Fruehan: *Metall. Trans. B*, 1989, vol. 20B, pp. 509-21.
10. M. Zamalloa and T. Utigard: Paper presented at *75th Steelmaking Conf.*, ISS-AIME, Toronto, 1992.
11. J.K. Yoon and M.K. Shin: *Proc. Int. Conf. on New Smelting Reduction and Near-Net-Shape Casting Technologies for Steel*, Pohang, Korea, 1990, pp. 97-106.
12. S. Kitamura and K. Okohira: *Iron Steel Inst. Jpn. Int.*, 1992, vol. 32, pp. 741-46.
13. Y. Ogawa and N. Tokumitsu: *Proc. 6th Int. Iron and Steel Congr.*, Iron and Steel Institute of Japan, Nagaya, 1990, pp. 147-52.
14. Y. Ogawa, D. Huin, H. Gaye, and N. Tokumitsu: *Iron Steel Inst. Jpn. Int.*, 1993, vol. 33, pp. 224-32.
15. H. Hirata, A. Matsuo, H. Katayama, H. Ishikawa, and H. Kajioka: *CAMP-ISIJ*, 1989, vol. 2, p. 172.
16. N. Tokumitsu, M. Matsuo, H. Katayama, H. Ishikawa, Y. Takamoto, and Y. Hayashi: *Proc. 7th Process Technology Conf.*, ISS-AIME, Toronto, 1988, pp. 99-107.
17. G.B. Wallis: *Proc. Symp. on Interactions between Fluids and Particles*, Institute of Chemical Engineers, London, 1962, vol. 9, pp. 9-16.
18. Z. Lin and R. Guthrie: *Trans. ISS*, 1995, May, pp. 67-73.
19. R. Frank, R. Selines, and Z. Du: Praxair Inc., Tarrytown, NY, unpublished research, 1990.
20. G.F. Hewitt: *Handbook of Multiphase Systems*, G. Hetsroni, ed, McGraw-Hill, New York, NY, 1982, pp. 2-15.
21. Y.T. Shah, B.G. Kelkar, S.P. Godbole, and W.D. Deckwer: *AIChEJ.*, 1982, vol. 28 (3), pp. 353-79.
22. K. Akita and F. Yoshida: *Ind. Eng. Chem. Proc. Des. Dev.*, 1973, vol. 21, p. 76.
23. H. Hikita, S. Asai, K. Tanigawa, K. Segawa, and M. Kitao: *Chem. Eng. J.*, 1980, vol. 20, p. 20.
24. P. Kozakevitch: *J Met.*, 1969, July, pp. 57-68.
25. G.A. Irons: *Ironmaking Steelmaking*, 1988, vol. 16, pp. 28-36.
26. L.R. Farias and G.A. Irons: *Metall. Trans. B*, 1986, vol. 17B, pp. 77-85.
27. G.S. Hanumanth, G.A. Irons, and S. Lafreniere: *Metall. Trans. B*, 1992, vol. 23B, pp. 753-63.
28. M. Schlichting, K. Downing, and E. Aukrust: AISI Direct Steelmaking, Pittsburgh, PA, unpublished research, 1991.
29. M.P. Fazleev, E.A. Ermakov, and O.S. Chekhov: *J. Appl. Chem. USSR*, 1985, vol. 58, pp. 32-37.
30. A.N. Khoze, Yu.I. Sharov, and Yu.V. O'Yachenko: *Fluid Mech. Sov. Res.*, 1980, vol. 9, pp. 94-97.
31. F. Yoshita and K. Akita: *AIChEJ.*, 1965, vol. 11, pp. 9-13.
32. Y.Y. Sheng and G.A. Irons: *Metall. Trans. B*, 1993, vol. 24B, pp. 695-705.
33. H. Katayama, T. Ibaraki, T. Ohno, M. Yamauchi, H. Hirata, and T. Inomoto: *Iron Steel Inst. Jpn. Int.*, 1993, vol. 33, pp. 124-32.
34. H. Katayama: Nippon Steel Corporation, Chiba, Japan, private communication, 1995.